JOURNAL OF Materials CHEMISTRY

Synthetic strategies for new inorganic oxide fluorides and oxide sulfates†

C. Greaves,* J. L. Kissick,‡ M. G. Francesconi,§ L. D. Aikens and L. J. Gillie

School of Chemistry, University of Birmingham, Birmingham, UK B15 2TT

Received 24th March 1998, Accepted 12th June 1998

The low temperature fluorination of low dimensional mixed metal oxides can be achieved in a variety of ways to provide new structures and modified electronic characteristics. The potential of these methods for the synthesis of new materials is considered, with particular reference to the fields of copper oxide superconductors and layered manganese oxide colossal magnetoresistance (CMR) phases; in both areas, careful structural and electronic control is necessary for optimised properties. The fluorination mechanisms are quite complex, and this paper describes the synthesis of three new oxide fluorides: $La_{1.9}Sr_{1.1}Cu_2O_5F_2$, $PbSr_2YCu_3O_6F_4$ and $La_{1.2}Sr_{1.8}Mn_2O_7F_2$, *via* processes which involve anion insertion, anion substitution and cation extraction. The use of a related strategy to incorporate more complex anions into oxides is also discussed, and the assimilation of SO_4^{2-} ions into Bi_2O_3 to give phases of composition $Bi_2O_{3-x}(SO_4)_x$ is described.

Introduction

The insertion of fluorine into mixed copper oxides to control carrier density and hence induce superconductivity, *e.g.* the fluorination of La_2CuO_4 to form $La_2CuO_4F_\delta$,[1] was established in the early days of high temperature superconductor research. However, only recently has the potential of fluorination for the synthesis of totally new superconducting structures been established. Although this synthetic strategy depends on the ability of fluorine to insert into fairly open structural frameworks, it is the variety of possible simultaneous processes which renders the method so useful for the design of new materials. Initial observations related to the fluorination of Sr_2CuO_3, using F_2 gas, to form superconducting $Sr_2CuO_2F_{2+\delta}$,[2] a process which involves not only insertion of fluorine and the substitution of fluorine for oxygen, but also—and more importantly—a structural rearrangement, which is illustrated schematically in Fig. 1. The potential of such fluorinations for the synthesis of new materials with useful properties is clearly demonstrated by this specific example, since the transformation indicated in Fig. 1 produces the CuO_2 layers which are essential for superconductivity in copper oxides but are absent in the Sr_2CuO_3 precursor oxide. Although Ca_2CuO_3 is isostructural with Sr_2CuO_3, it is interesting to note that the fluorinated product, $Ca_2CuO_2F_{2+\delta}$, is structurally different from $Sr_2CuO_2F_{2+\delta}$, although anion rearrangement again occurs to produce CuO_2 sheets.[3] A variety of other fluorinating agents, *e.g.* NH_4F, CuF_2, ZnF_2, XeF_2, AgF_2, can be used to induce very similar transformations, and differ mainly in their oxidising power and ability to produce uncontaminated products.[4]

$Sr_2CuO_2F_{2+\delta}$ is the $n=1$ member of a Ruddlesden–Popper type series of compounds which can be represented as $Sr_2Ca_{n-1}Cu_nO_{2n}F_{2+\delta}$. Using high pressure methods, the $n=2$ and $n=3$ members have now been synthesised with superconducting transitions at 99 and 111 K respectively.[5] The variety of structural effects is demonstrated by the insertion of fluorine into reduced $YBa_2Cu_3O_{6+\delta}$,[6] Fig. 2. Whereas the insertion process appears to be related to that occurring in Sr_2CuO_3, in this case no structural transformation or F/O exchange occurs, and $YBa_2Cu_3O_6F_2$ is formed with $T_c=94$ K.

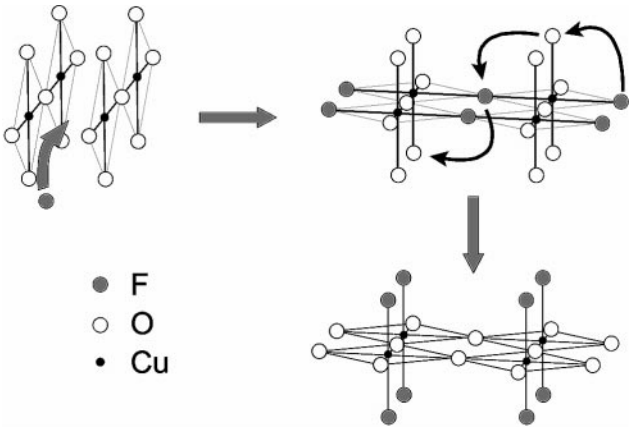

Fig. 1 Schematic representation of the fluorination of Sr_2CuO_3, which contains chains of corner-linked CuO_4 units, to form $Sr_2CuO_2F_{2+\delta}$ with CuO_2 sheets and apical Cu–F bonds.

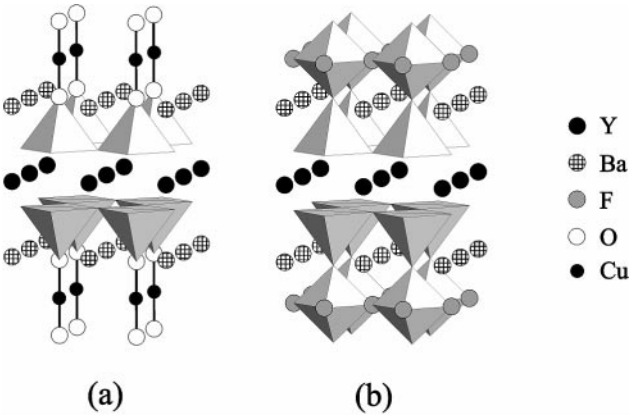

Fig. 2 The structures of (a) $YBa_2Cu_3O_6$ and (b) $YBa_2Cu_3O_6F_2$ highlighting the Cu coordination polyhedra.

As described in recent reviews of low temperature fluorination processes,[7,8] and demonstrated by the specific examples described above, fluorine insertion reactions can be associated with four different processes: (i) substitution of an

†Basis of the presentation given at Materials Chemistry Discussion No. 1, 24–26 September 1998, ICMCB, University of Bordeaux, France.

‡Present address: Department of Chemistry, Oregon State University, Corvallis, OR97331-4003, USA.

§Present address: Department of Chemistry, University of Nottingham, Nottingham, UK NG7 2RD.

O^{2-} ion by an F^- ion; (ii) replacement of one O^{2-} ion by two F^- ions; (iii) insertion of F^- ions into interstitial sites within the structure; and (iv) structural rearrangement induced by a significant O/F site preference energy. Processes (i) and (iii) have associated charge balance consequences, and respectively cause reduction or oxidation of the structural framework. The synthesis of oxide fluorides is therefore of value for the control of both electronic and structural properties of materials, and may be of importance for the fabrication of new materials where the interplay of such factors is of paramount importance, *e.g.* for high temperature superconductors and magnetic (colossal magnetoresistance, CMR) materials.

In this paper, the synthesis and structures of three new oxide fluoride materials are reported. Two were derived from oxides related to superconductors—$La_{1.9}Sr_{1.1}Cu_2O_6$ and $Pb_2Sr_2YCu_3O_8$—and the other was obtained from fluorination of the two-dimensional CMR phase $La_{1.2}Sr_{1.8}Mn_2O_7$. The precursor oxides all appeared structurally suitable for fluorine insertion since they contain adjacent rocksalt (MO) layers similar to those in Sr_2CuO_3 and between which the excess F ions reside in $Sr_2CuO_2F_{2+\delta}$. At present, little attention has been devoted to determining the physical characteristics of these materials, and here we present only structural data. However, both copper containing phases have the structural requirements to support superconductivity. The study has been extended to examine the possibility of using a related synthetic strategy to incorporate SO_4^{2-} anions into oxide frameworks, and we compare the results of heating Bi_2O_3 with $(NH_4)_2SO_4$ with fluorinations involving NH_4F.

Experimental

Synthesis

$La_{1.9}Sr_{1.1}Cu_2O_6$ was prepared conventionally from a mixture of high purity La_2O_3, $SrCO_3$ and CuO by heating in air at 1075 °C for three periods of 15 h, with a thorough grinding between heatings. Although a variety of fluorination procedures may be employed for materials of this type,[9] this study used an intimate mixture of $La_{1.9}Sr_{1.1}Cu_2O_6$ and excess NH_4F (molar ratio 1 : 5, 350 °C for 20 h). The process was repeated four times (overall molar ratio of 1:20) to achieve maximum fluorine uptake.

The sample of $Pb_2Sr_2YCu_3O_8$ was synthesised from a precursor obtained by heating a mixture of $SrCO_3$, Y_2O_3 and CuO at 900 °C for 5 h in flowing O_2. The stoichiometric amount of PbO was then mixed with the precursor and heated at 900 °C in N_2 for three periods of 12 h. Fluorination was achieved by mixing with NH_4F (molar ratio 1 : 6) and heating in air or flowing N_2 at 350 °C for 8 h. Similar, but not identical, products have been obtained using F_2 gas or CuF_2 as fluorinating agents.

$La_{1.2}Sr_{1.8}Mn_2O_7$ was synthesised from an intimate stoichiometric mixture of La_2O_3, $SrCO_3$ and MnO_2. In accordance with previous accounts,[10] a small amount of Bi_2O_3 (0.05 mole per formula unit) was added as a flux which volatilises during the subsequent heat treatments: 12 h at 900 °C, 12 h at 1200 °C and 50 h at 1300 °C with intermediate grinding. Fluorination was investigated using CuF_2 as fluorinating agent. Five heat treatments (8 h at 220 °C) were given with the following amounts of CuF_2 being added at each stage to achieve eventual saturation: 1.5, 0.5, 0.25, 0.1, and 0.1 mole equivalents.

The formation of a material with stoichiometry $Bi_2O_{2.86}(SO_4)_{0.14}$ was achieved by heating an intimate mixture of Bi_2O_3 and $(NH_4)_2SO_4$ at 750 °C for two periods of 16 h.

Characterisation

Stuctural characterisation was achieved using Rietveld refinement of X-ray powder diffraction (XRD) data (Siemens D5000, transmission mode, primary beam monochromator, 8° PSD) and neutron powder diffraction data (POLARIS, ISIS, Rutherford Appleton Laboratory). The programs FULLPROF[11] and GSAS[12] were used for refinements using XRD and neutron diffraction data, respectively. The distribution of O^{2-} and F^- ions on the anion sublattices were investigated using Madelung energy calculations.[13] Although bond valence sum calculations[14] were performed, they were found to be of little value owing to several factors, especially the mixed oxidation states for Cu and Mn, and cation disorder (La/Sr mixing in the fluorinated products of $La_{1.9}Sr_{1.1}Cu_2O_6$ and $La_{1.2}Sr_{1.8}Mn_2O_7$, and partial occupancy of the Pb sites in the product from $Pb_2Sr_2YCu_3O_8$).

Results and discussion

Fluorination of $La_{1.9}Sr_{1.1}Cu_2O_6$

The Ruddlesden–Popper phases with general formula $(Ln,A)_3Cu_2O_6$ (Ln = lanthanide, A = Sr,Ca), Fig. 3(a), have rarely demonstrated superconducting behaviour owing to the difficulty in achieving adequate electronic control.[15] An exploration of the possibility of using fluorination to achieve such control has previously been described,[9] and the most pronounced structural change observed was a significant expansion along *c*. In the present study, the unit cell of $La_{1.9}Sr_{1.1}Cu_2O_6$ [tetragonal; $a = 3.851(1)$ Å, $c = 20.048(6)$ Å] expanded to an orthorhombic cell (*Immm*) with $a = 3.8540(2)$ Å, $b = 3.9200(2)$ Å, $c = 21.425(1)$ Å. Chemical analysis has indicated that under the fluorination conditions used, the Cu oxidation state increases only slightly (to approximately 2.1) and approximately 2F per formula unit are incorporated into the structure. The predominant incorporation mechanism therefore appeared to involve the replacement of one O^{2-} by $2F^-$ ions per formula unit. Three phases were present in the sample: the major fluorinated product, and two decomposition products, one related to fluorite (probably La-doped SrF_2) and CuO. In order to obtain an indication of the nature of the fluorine insertion, and whether structural rearrangement had occurred, structural analysis was performed using XRD data, and the fitted profile is shown in Fig. 4. Structural data for the principal phase are given in Table 1 and the structure is shown in Fig. 3(b). The atoms O1 and O2 are equatorially bonded to Cu whilst O3 and F2 occupy apical positions. To simplify the refinement, three thermal parameters were refined: one for La/Sr, one for Cu and one for O/F. The presence of a fluoride-containing impurity reduced the value of chemical analysis for determining the fluorine content in the primary phase, and therefore no chemical constraints were applied to anion occupancies. Since XRD

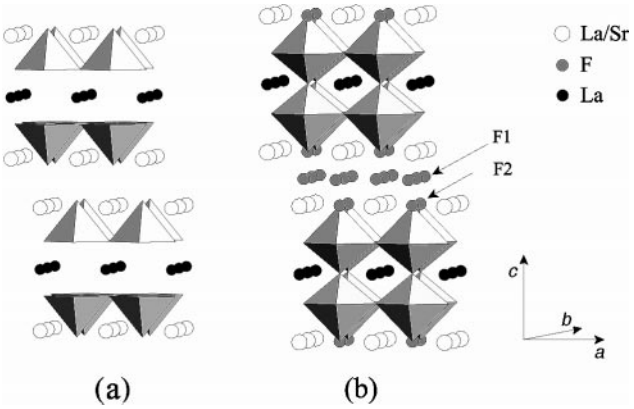

Fig. 3 The structures of (a) $La_{1.9}Sr_{1.1}Cu_2O_6$ and (b) $La_{1.9}Sr_{1.1}Cu_2O_5F_2$ showing the CuO_5 square pyramids and CuO_5F octahedra. In $La_{1.9}Sr_{1.1}Cu_2O_5F_2$, Cu is coordinated equatorially by O1 and O2 and has apical O3 and F2 atoms.

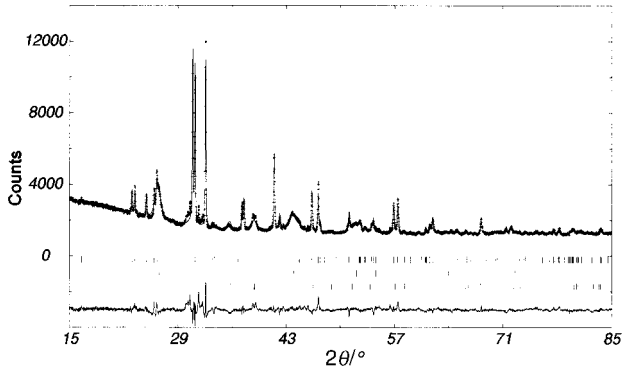

Fig. 4 Observed, calculated and difference XRD profiles of $La_{1.9}Sr_{1.1}Cu_2O_5F_2$ (upper tick marks), $(La,Sr)F_{2+x}$ (middle tick marks) and CuO (lower tick marks).

Table 1 Refined parameters, $La_{1.9}Sr_{1.1}Cu_2O_5F_2$

Atom	x/a	y/b	z/c	B/Å^2	Cell occupancy
La	0	0	0	2.4(1)	2
La/Sr	0	0	0.1775(2)	2.4(1)	1.8/2.2
Cu	0	0	0.5873(5)	2.0(2)	4
O1	0	0.5	0.093(2)	3.0(5)	4
O2	0.5	0	0.084(2)	3.0(5)	4
O3	0	0	0.5	3.0(5)	2
F1	0.5	0	0.253(2)	3.0(5)	2.4(2)
F2	0	0	0.677(2)	3.0(5)	1.8(2)

Immm; $a=3.8540(2)$ Å, $b=3.9200(2)$ Å, $c=21.425$ Å; $R_{wp}=5.54\%$, $R_{exp}=2.29\%$.

cannot differentiate between O and F ions, the site distribution shown in Table 1 was derived from Madelung energy calculations.[13] There is, however, only a small energy preference (165 kJ mol^{-1}) for the O3 site to be occupied by O rather than F, and for this material the distribution of O^{2-} and F^- ions must be regarded as uncertain. The high thermal parameters are thought to be indicative of a high level of local disorder which is to be expected given the partial occupancy of both the interstitial F1 site and the apical F2. Bond distances to Cu are Cu–O1 = 1.93(1) Å [×2], Cu–O2 = 1.96(1) Å [×2], Cu–O3 = 1.87(1) Å, Cu–F2 = 1.92(4) Å.

According to the XRD site occupancies, the fluorinated product has the composition $La_{1.9}Sr_{1.1}Cu_2O_5F_{2.1(2)}$, which agrees well with chemical analysis. On the basis of the Madelung energies, O^{2-} ions preferentially occupy the anion positions between the Cu positions which are vacant in $La_{1.9}Sr_{1.1}Cu_2O_6$, and a disordered array of F^- ions provides partial filling of the apical Cu coordination sites and the interstitial (fluorite block) sites. Redistribution of the anions therefore occurs to form the Cu–O–Cu links shown in Fig. 3(b), which are unusual and probably form due to the large Cu–Cu separation [3.712(4) Å][16] in the precursor oxide. Interestingly, only a small expansion occurs [to 3.74(2) Å] when O^{2-} ions form Cu–O–Cu links. Although very small Meissner signals have been observed in some samples,[9] in general the materials appear to be underdoped and further attention to electronic control is necessary if bulk superconductivity is to be realised.

Fluorination of $Pb_2Sr_2YCu_3O_8$

The structure of $Pb_2Sr_2YCu_3O_8$ (orthorhombic, *Cmmm*, $a=5.393$ Å, $b=5.431$ Å, $c=15.733$ Å),[17] is shown in Fig. 5(a). It has quite large channels in the vicinity of the linearly coordinated Cu^I linking layers, and it also has Pb/SrO rocksalt regions similar to those found in the Ruddlesden–Popper series of compounds. Electronic control *via* the partial replacement of Y by Ca induces superconductivity with $T_c=70$ K.[18] It has

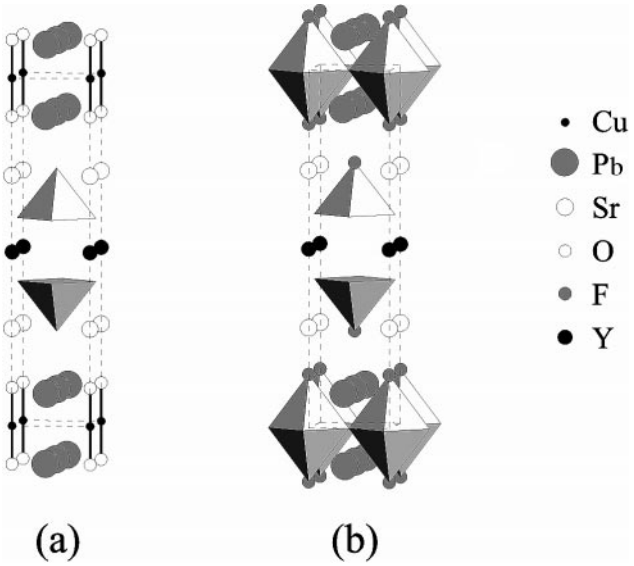

Fig. 5 The structures of (a) $Pb_2Sr_2YCu_3O_8$ and (b) $PbSr_2YCu_3O_6F_4$. In $PbSr_2YCu_3O_6F_4$, Cu1 is octahedrally coordinated by four O2 (equatorial) and two F2 (apical); Cu2 is square pyramidally coordinated by four O1 and one F1.

been found that the results of fluorination of this phase depend on the fluorination method employed; here, fluorination by only NH_4F is considered. XRD revealed substantial structural changes had occurred within the primary phase to give a tetragonal structure [*P*4/*mmm*, $a=3.8601(2)$ Å, $c=17.062(3)$ Å], and a fluorite related phase with $a=5.779(1)$ Å (GSAS refinement, see below) was produced. This phase has been assumed to be PbF_2 (or a closely related analogue) although the unit cell is slightly smaller than that reported in the literature [5.925(4) Å];[19] structure refinement was consistent with the stoichiometry PbF_2. Neutron powder diffraction suggested the primary phase to have the composition $PbSr_2YCu_3O_6F_4$ with the structure shown in Fig. 5(b); this is consistent with the substantial expansion observed along [001]. The fitted profile is shown in Fig. 6 and refined structural parameters are given in Table 2. The distribution of O^{2-} and F^- ions within the anion framework was deduced from Madelung energy calculations.[13] The formula $PbSr_2YCu_3O_6F_4$ implies oxidation of the oxide which can be considered to occur either at Cu ions (to give formally two Cu^{2+} and one Cu^{3+}) in the unit cell or at the Pb sites ($3Cu^{2+}$ ions with $0.5Pb^{2+}$ and $0.5Pb^{4+}$). Irrespective of the model assumed for charge balance, Madelung energy calculations strongly supported the anion distribution shown in Table 2 and Fig. 5(b). Table 3 lists values of the Madelung energy for various possible anion distributions assuming oxidation of the Cu1 site to Cu^{3+}. Bond distances to Cu are: Cu1–O2 = 1.944(1) Å [×4],

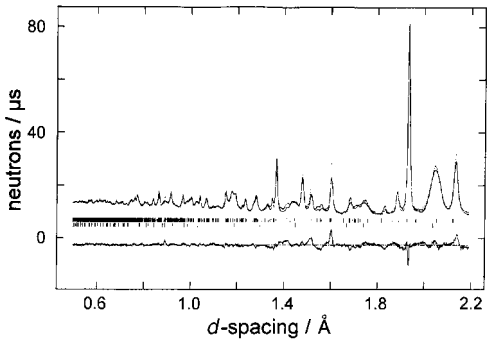

Fig. 6 Observed, calculated and difference neutron diffraction profiles of $PbSr_2YCu_3O_6F_4$ (upper tick marks) and PbF_2 (lower tick marks).

Table 2 Refined structural parameters, $PbSr_2YCu_3O_6F_4$

Atom	*x*/*a*	*y*/*b*	z/c	*B*/Å^2	Cell occupancy
Pb	0.5	0.5	0.0957(5)	0.47(5)	1
Sr	0	0	0.2875(7)	3.4(2)[a]	2
Y	0	0	0.5	0.47(5)	1
Cu1	0	0	0	0.47(5)	1
Cu2	0.5	0.5	0.3977(4)	0.47(5)	2
O1	0.5	0	0.4122(3)	1.00(6)	4
O2	0.5	0	0.0138(6)	1.00(6)	2
F1	0.408(2)	0.408(2)	0.2702(7)	1.00(6)	2
F2	0.063(1)	0.063(1)	0.1507(9)	1.00(6)	2

*P*4/*mmm*; $a=3.8601(2)$ Å, $c=17.062(3)$ Å; $R_{wp}=2.84\%$, $R_{exp}=0.78\%$.
[a]Equivalent to $B_{11}=B_{22}=1.34(15)$ Å^2; $B_{33}=7.5(7)$ Å^2.

Table 3 Madelung energy for various anion distributions in $PbSr_2YCu_3O_6F_4$

Distribution of oxygen (O) and fluorine (F)[a]				Madelung energy/ kJ mol^{-1}
O1	O2	F1	F2	
O	O	F	F	33 149
F	O	O	O	20 113
O	F	F	O	31 737
O	F	O	F	30 364

[a]See Table 2 and Fig. 3 for site descriptions.

Cu1–F2 = 2.57(2) Å [×2]; Cu2–O1 = 1.930(1) Å [×4], Cu2–F1 = 2.20(2) Å.

Fluorine enters the $Pb_2Sr_2YCu_3O_8$ lattice in the vicinity of the PbO–Cu–PbO regions (Fig. 5) and causes structural rearrangement to provide octahedrally coordinated Cu with a new CuO_2 plane and two apical fluorine ions. The structure therefore appears to contain two distinct regions which are both capable of supporting superconductivity: a single layer of corner linked CuO_4F_2 octahedra and a double layer of CuO_4F square pyramids. In this fluorination, several interesting chemical processes seem to be involved: (i) F^- for O^{2-} substitution within the PbO layers; (ii) rearrangement of the O^{2-} ions to create new CuO_2 layers; and (iii) overall oxidation of the Cu–O framework caused primarily by abstraction of 50% of the Pb^{2+} cations.

Certain structural features indicated in Table 2, *viz.* the thermal parameter for Sr and the displacements of F1 off the ideal (1/2,1/2,*z*) position, are attributed to structural variations associated with the presence of 50% vacancies on the Pb sites. It is believed that the overall energetics of the reaction may be influenced by the high lattice energy of the PbF_2 phase formed. It is particularly interesting, and initially surprising, to note that the fluorination reaction, and associated oxidation, occurs in flowing N_2. Under these conditions, the oxidation within the solid is presumably balanced by reduction of NH_4^+ ions to NH_3 and H_2 and it is our view that this unusual reaction can be rationalised by lattice energy considerations. In particular, the extraction of Pb from the solid to form the fluorite-related PbF_2 is the principal driving force as indicated by the calculated Madelung energies: $Pb_2Sr_2YCu_3O_8$ (32 794 kJ mol^{-1}), $PbSr_2YCu_3O_6F_4$ (33 149 kJ mol^{-1}) and PbF_2 (2 793 kJ mol^{-1}).

Fluorination of $La_{1.2}Sr_{1.8}Mn_2O_7$

Fluorination of $La_{1.2}Sr_{1.8}Mn_2O_7$ [tetragonal, $a=3.8833(1)$ Å, $c=20.142(1)$ Å] using CuF_2 was found to result in gradual evolution of a new material which was characterised by large contraction in the *ab* plane and expansion along *c*: $a=3.7694(1)$ Å, $c=23.379(1)$ Å. Although the use of CuF_2 resulted in CuO as a second phase, it was used in preference to NH_4F since it produced a single phase fluorinated product of the manganese oxide precursor. This presumably relates to the greater oxidising power of CuF_2. At the low temperature of the fluorination, negligible intermixing of Cu and Mn was anticipated, and this was supported in the subsequent structure refinement based on XRD data, which indicated that the phase fraction of CuO was in accordance with that mixed with the precursor. The refined structure clearly demonstrated the insertion of F^- ions into interstitial sites between the two (La/Sr)O rocksalt layers as shown in Table 4 and Fig. 7. The fitted XRD profile is shown in Fig. 8. The change in unit cell size is consistent with insertion of F^- ions between layers perpendicular to [001], with concomitant oxidation of Mn. The structure supports the incorporation of two F^- ions per $La_{1.2}Sr_{1.8}Mn_2O_7$ formula unit (average Mn oxidation state +3.4) to produce $La_{1.2}Sr_{1.8}Mn_2O_7F_2$ (average Mn oxidation state +4.4). Madelung energy calculations support the

Table 4 Refined structural parameters, $La_{1.2}Sr_{1.8}Mn_2O_7F_2$

Atom	*x*/*a*	*y*/*b*	*z*/*c*	*B*/Å^2	Cell occupancy
La/Sr1	0	0	0.5	0.9(1)	1.27(6)/0.73(6)
La/Sr2	0	0	0.3205(2)	0.9(1)	1.13(6)/2.87(6)
Mn	0	0	0.0856(6)	0.6(2)	4
O1	0	0	0	1.3(3)	2
O2	0	0.5	0.087(1)	1.3(3)	8
O3	0	0	0.831(1)	1.3(3)	4
F1	0.5	0	0.25	1.3(3)	4

*I*4/*mmm*; $a=3.7694(1)$ Å, $c=23.379(1)$ Å; $R_{wp}=3.42\%$, $R_{exp}=1.10\%$.

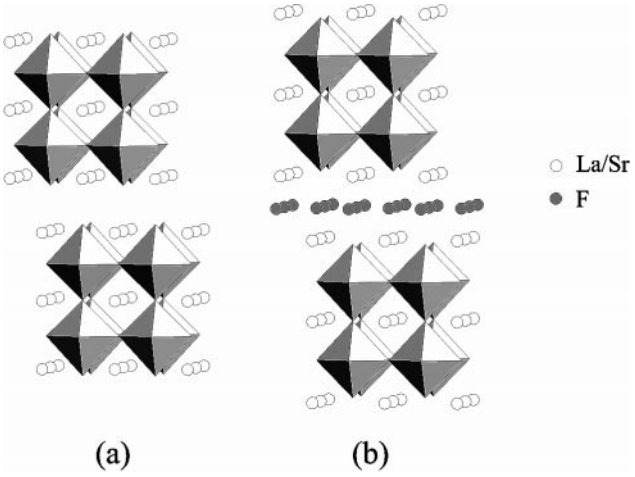

Fig. 7 The structures of (a) $La_{1.2}Sr_{1.8}Mn_2O_7$ and (b) $La_{1.2}Sr_{1.8}Mn_2O_7F_2$. In $La_{1.2}Sr_{1.8}Mn_2O_7F_2$, Mn is octahedrally linked to O1, O3 and four O2. Layers of octahedra are formed by linking through the O2 atoms, and the layers are linked *via* O1. F atoms occupy sites between the (La/Sr)O rocksalt layers.

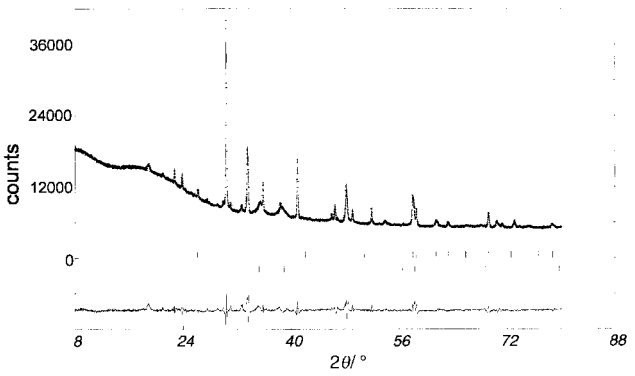

Fig. 8 Observed, calculated and difference XRD profiles of $La_{1.2}Sr_{1.8}Mn_2O_7F_2$ (upper tick marks) and CuO (lower tick marks).

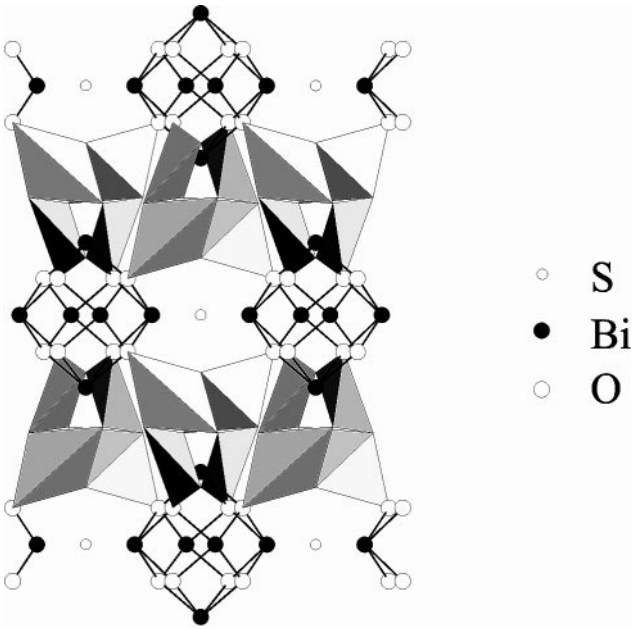

Fig. 9 Structure of $Bi_{14}O_{20}SO_4$. The BiO_4 trigonal bipyramids are shown as solid polyhedra and the BiO_4 square pyramids are represented by the Bi–O bonds. Only the central S atoms of the SO_4 groups are shown.

location of F^- ions in the interstitial site (44 718 kJ mol^{-1}) compared with the most likely alternative where it would be bonded to Mn in an apical position (the O3 site; 42 130 kJ mol^{-1}). As in previous studies,[10] the La/Sr distribution shows a preference of Sr^{2+} ions for the nine-coordinate site in the rocksalt layers (La/Sr2 in Table 4) rather than the twelve-coordinate perovskite site (La/Sr1). The bonds to Mn in $La_{1.2}Sr_{1.8}Mn_2O_7F_2$ are Mn–O1 = 2.00(1) Å, Mn–O2 = 1.885(1) Å [×4], Mn–F1 = 1.96(1) Å and differ markedly with respect to the equatorial bonds (Mn–O2) compared with the precursor oxide, for which the comparable distances are respectively 1.97, 1.94 and 1.98 Å.[10] This is consistent with oxidation of the Mn–O framework, but a significantly more distorted environment is observed in the highly oxidised fluorinated material. The electrical and magnetic properties of this material have yet to be determined but are of particular interest given the CMR behaviour of $Tl_2Mn_2O_7$,[20] which also contains Mn in a high formal oxidation state.

Incorporation of SO_4^{2-} ions into Bi_2O_3

Given the successful use of NH_4F as a means of inserting F^- ions into oxide frameworks, the possible use of $(NH_4)_2SO_4$ for incorporating SO_4^{2-} ions is being explored. Although the decomposition temperature of $(NH_4)_2SO_4$ is only 235 °C, very simple heat treatments of Bi_2O_3–$(NH_4)_2SO_4$ mixtures at 750 °C have been found to result in new bismuth oxide-sulfates without any significant loss of the sulfate anions. Details of the structure of one of the phases synthesised, $Bi_{14}O_{20}(SO_4)$, have been reported elsewhere,[21] and here only the principal features are highlighted. During synthesis, SO_4^{2-} groups enter the Bi_2O_3 structure and a new structure forms. The body-centred tetragonal unit cell [$I4/m$; $a = 8.664(1)$ Å, $c = 17.282(2)$ Å] is a commensurate superstructure of the cubic fluorite subcell of δ-Bi_2O_3 (a_o): $a = (10^{1/2}/2)a_o$, $c = 3a_o$. The unit cell is marked by SO_4^{2-} groups at the corners and body centre, and contains a Bi–O framework of BiO_4e (e = lone pair of electrons) trigonal bipyramids and square pyramids. Unlike in δ-Bi_2O_3, where the O^{2-} ions are disordered, complete order of the oxygen sublattice is observed at 300 K: the square pyramids are aggregated into Bi_6O_8 clusters and the trigonal bipyramids are corner linked to form layers as shown in Fig. 9. This material is just one of a new class of structurally related phases, which are currently under investigation and are synthesised from different Bi_2O_3 : $(NH_4)_2SO_4$ ratios.

Conclusions

Low temperature fluorination of mixed metal copper oxides containing fairly open structural frameworks can result in a variety of structural effects involving fluorine insertion, fluorine substitution, structural rearrangement and cation extraction. In this way, not only can new structural elements capable of supporting superconductivity be created, but additional means of electronic control are also possible. The synthesis methods described have potential for the design and synthesis of new superconducting materials, but in general the thermal stability of such oxide fluorides is limited so that processing of the resultant materials will be difficult. The fluorination of the magnetic phase $La_{1.2}Sr_{1.8}Mn_2O_7$ to form $La_{1.2}Sr_{1.8}Mn_2O_7F_2$ demonstrates that the strategy may also be of value in the synthesis of new magnetic materials where the properties are also influenced strongly by structural and electronic considerations. The potential of new oxide sulfates such as $Bi_{14}O_{20}(SO_4)$ has yet to be established, but given the useful catalytic and ionic conduction properties of bismuth oxides and doped variants, the new structural characteristics induced by the incorporation of oxyanions such as SO_4^{2-} may prove to be of importance.

We thank EPSRC for the provision of neutron diffraction facilities and for financial support.

References

1 B Chevalier, A. Tressaud, B. Lepine, K. Amine, J. M. Dance, L. Lozano, E. Hickey and J. Etourneau, *Physica C*, 1990, **167**, 97.
2 M. Al-Mamouri, C. Greaves, P. P. Edwards and M. Slaski, *Nature* (*London*), 1994, **369**, 382.
3 M. Al-Mamouri, P. P. Edwards, C. Greaves, P. R. Slater and M. Slaski, *J Mater. Chem.*, 1995, **5**, 913.
4 M. G. Francesconi, P. R. Slater, J. P. Hodges, C. Greaves, P. P. Edwards, M. Al-Mamouri and M. Slaski, *J. Solid State Chem.*, 1998, **135**, 17.
5 T. Kawashima, E. Matsui and E. Takayama-Muromachi, *Physica C*, 1996, **257**, 313.
6 R. V. Shpanchenko, M. G. Rozova, A. M. Abakumov, E. I. Ardashnikova, M. L. Kovba, S. N. Putilin, E. V. Antipov, O. I. Lebedev and G. Van Tendeloo, *Physica C*, 1997, **280**, 272.
7 M. G. Francesconi and C. Greaves, *Supercond. Sci. Technol.*, 1997, **10**, A29.
8 C. Greaves and M. G. Francesconi, *Curr. Opin. Solid State Mater. Sci.*, 1998, **3**, 132.
9 P. R. Slater, J. P. Hodges, M. G. Francesconi, C. Greaves and M. Slaski, *J. Mater. Chem.* 1997, **7**, 2077.
10 R. Seshadri, C. Martin, A. Maignan, M. Hervieu, B. Raveau and C. N. R. Rao, *J. Mater. Chem.*, 1996, **6**, 1585.
11 J. Rodriguez-Cavajal, FULLPROF, version 3.2, based on the original code by D. B. Wiles, and R. A. Young, *J. Appl. Crystallogr.*, 1981, **14**, 149.
12 A. C. Larson and R. B. Von Dreele, General Structure Analysis System, University of California, 1994.
13 J. W. Weenk and H. A. Harwig, *J. Phys. Chem. Solids*, 1977, **38**, 1047.
14 I. D. Brown and D. Altermatt, *Acta Crystallogr.*, *Sect. B*, 1985, **41**, 244.
15 R. J. Cava, B. Batlogg, R. B. van Dover, J. J. Krajewski, J. V. Waszczak, R. M. Fleming, W. F. Peck Jr., L. W. Rupp Jr., P. Marsh, A. C. W. P James and L. F. Schneemeyer, *Nature* (*London*) 1990, **345**, 602.
16 R. C. Lobo, Ph.D. Thesis, University of Birmingham, 1990.
17 R. J. Cava, M. Marezio, J. J. Krajewski, W. F. Peck Jr., A. Santoro and F. Beech, *Physica C*, 1989, **157**, 272.

18 R. J. Cava, B. Batlogg, J. J. Krajewski, L. W. Rupp, L. F. Schneemeyer, T. Siegrist, R. B. van Dover, P. Marsh, W. F. Peck Jr., P. K. Gallagher, S. H. Glarum, J. H. Marshall, R. C. Farrow, J. V. Waszczak, R. Hull and P. Trevor, *Nature* (*London*), 1988, **336**, 211.
19 Y. Ito and K. Koto, *Solid State Ionics*, 1983, **9–10**, 527.
20 Y. Shimakawa, Y. Kubo and T. Manako, *Nature* (*London*), 1996, **379**, 53.
21 M. G. Francesconi, A. L. Kirbyshire, C. Greaves, O. Richard and G. Van Tendeloo, *Chem. Mater.*, 1998, **10**, 626.

Paper 8/04447C